PAPER

Study of interactions between Brønsted acids and triethylphosphine oxide in solution by ^{31}P NMR: evidence for 2 : 1 species†

Elisabet Pires [ID] and José M. Fraile [ID] *

The variation of the ^{31}P chemical shift of triethylphosphine oxide in CDCl$_3$ solution with a series of Brønsted acids at different molar ratios allows the determination of the value for the 1 : 1 species ($\delta_{1:1}$), which is much lower than the reported value at infinite dilution. This value correlates with the pK_a of the acid in two zones, for acids stronger and weaker than TEPO–H$^+$. The acid strength also controls the exchange rate in solution. The evolution of the chemical shift at high acid/TEPO molar ratios indicates the existence of a second TEPO–acid interaction, which is also dependent on the acid strength. This interaction is much more favorable in the case of a diacid, which shows chemical shift higher than expected for its pK_{a1} value.

Introduction

Triethylphosphine oxide (TEPO) was classically used as a probe molecule to characterize the electrophilic properties of solvents, taking advantage of its wide range of chemical shifts in ^{31}P NMR spectroscopy due to the deshielding effect on phosphorus by inductive effect. This was the base of an empirical solvent parameter, known as Gutmann's acceptor number (AN),[1] determined from the extrapolated chemical shift at infinite dilution of TEPO in the corresponding solvent. The phosphorus atom is not shielded by the positive charge, as it occurs in phosphines, making it highly sensitive to hydrogen bonding.[2] Since then, this method has been employed to characterize liquids with acidic properties, such as boron compounds used as Lewis acid catalysts,[3] and different types of ionic liquids with Brønsted[4] or Lewis[5,6] acidity, and phosphine oxides have been proposed as descriptors for halogen bonds.[7] A similar methodology, taking the chemical shift at infinite dilution, has been applied for the determination of acidity by ^{13}C NMR using mesityl oxide as the probe molecule.[8]

The ^{31}P NMR method with TEPO was soon adapted for the characterization of solids, creating a scale of global acidity.[9] Although TEPO was initially used, in analogy with the AN determination, other trialkylphosphine oxides (PO), such as trimethylphosphine oxide (TMPO) or tributylphosphine oxide (TBPO), have also been utilized for this purpose, with the aim of

Instituto de Síntesis Química y Catálisis Homogénea (ISQCH), Facultad de Ciencias, CSIC-Universidad de Zaragoza, Pedro Cerbuna 12, E-50009 Zaragoza, Spain. E-mail: josem.fraile@csic.es

† Electronic supplementary information (ESI) available: NMR spectra and fitted graphs for all the acids. See DOI: 10.1039/d0cp03812a

getting information not only about acid strength, but also the acid type (Brønsted or Lewis), the location and the amount of acid sites.[10,11]

However, the deshielding effect on trialkylphosphine oxides is measured under very different conditions in both methods. In solution, the high dilution conditions and the extrapolation to calculate Gutmann's AN make the acid/PO ratio nearly ∞, considering the acid as a solvent, whereas on solids, the amount of PO used is close to or slightly below the stoichiometric 1 : 1 ratio. Surprisingly, the studies of acids in solution under similar quasi-stoichiometric conditions are rather scarce.

Myers *et al.* characterized BF$_3$, TMSOTf (trimethylsilyl triflate) and mixtures of both in CDCl$_3$ by using TEPO in amounts from 0.25 equivalents to a slight excess over the Lewis acids.[12] Several interesting features were observed, such as the presence of several species with different Lewis acidity and the rather slow exchange of TEPO, as the ^{31}P signals for free and coordinated TEPO did not collapse into one single peak at room temperature.

Koito *et al.* have studied the acidity of different Lewis acids, mainly metal triflates and chlorides, in D$_2$O with acid/TMPO molar ratios in the range of 0.5 to 8.[13,14] Several catalysts did not show any important deshielding effect on TMPO, showing that most of the TMPO was not coordinated to the Lewis acid. On the contrary, Sc(OTf)$_3$, In(OTf)$_3$ and ScCl$_3$ showed an important deshielding effect, which is in agreement with their higher catalytic activity in water. The number of signals and the line width at different acid/TMPO ratios were used to determine the rather slow exchange rates.

Very recently, Diemoz and Franz have used a TEPO ^{31}P chemical shift to create a scale of the hydrogen-bond activating effect of different organocatalysts, including alcohols, phenols,

silanols, carboxylic acids, ureas, phosphoric acids and boronic acids.[15] In this case, a catalyst/TEPO molar ratio of 3 was consistently used to get the saturation ^{31}P chemical shift value. However, this study was restricted to rather weak acids.

Thus, a fair comparison of the ^{31}P chemical shifts of analogous homogeneous and heterogeneous catalysts is difficult. This is due to the very different conditions in which the ^{31}P chemical shifts are measured. In this manuscript, we present our results of ^{31}P NMR spectroscopy in solution with TEPO as a probe molecule and different Brønsted acids that can serve as homogeneous analogues of heterogeneous catalysts.

Experimental

Acetic acid (Acros, 99.8%), formic acid (Sigma-Aldrich, 98%), 2,2,2-trifluoroethanol (Fluorochem, 99%), phenylphosphonic acid (Acros, 98%), trifluoroacetic acid (Sigma-Aldrich, 99%), methanesulfonic acid (Sigma-Aldrich, 99.5%), p-toluenesulfonic acid (Sigma-Aldrich, 98.5%), trifluoromethanesulfonic acid (Fluka, 98%), dimethylmalonic acid (Aldrich, 98%) and α,α,α-trifluorotoluene (Alfa Aesar, 99%) were used without further purification. CDCl$_3$ and methanol-d_4 (Aldrich, 99.8% D) were kept at 4 °C and used as received. Triethylphosphine oxide (Aldrich, 99%) was kept and manipulated in a glove box under Ar.

Preparation of the samples

In a 10 mL volumetric flask, a solution of 100 mg of TEPO in CDCl$_3$ or MeOH-d_4 was prepared and then treated with 4 Å molecular sieves for 24 h. For liquid acids, 1 mL of the TEPO solution was placed in an NMR tube, and the appropriate amount of acid was added using a micropipette. For solid acids, the exact amount of acid was weighed in a glass tube, and then 1 mL of the TEPO solution was added. The solution was then stirred until total acid dissolution. The solution was then placed in an NMR tube. In the case of triflic and trifluoroacetic acid samples, 31 μL of α,α,α-trifluorotoluene were also added as an internal standard. In all of the cases, the NMR tube was purged with Ar and the sample was allowed to equilibrate at room temperature before NMR recording.

For the preparation of the adducts, a solution of 250 mg of TEPO in anhydrous CH$_2$Cl$_2$ or CH$_3$OH was prepared in a 25 mL volumetric flask. Then, p-toluenesulfonic acid or phenylphosphonic acid was weighed in a 10 mL round bottom flask, and the adequate volume of TEPO solution was added. The solution was stirred under argon for 30 min, and the solvent was removed by vacuum distillation. Dried KBr was added to the viscous liquid, and the solid was placed in a 4 mm ZrO$_2$ rotor.

NMR experiments

Solution NMR spectra were recorded at 300 K in a Bruker Avance 400 spectrometer equipped with a 5 mm QNP probe at resonance frequencies of 400.16, 161.99 and 376.49 MHz for ^{1}H, ^{31}P and ^{19}F, respectively. ^{31}P spectra (30° pulse 12 μs, 128 scans) were recorded under ^{1}H decoupling, and referenced using the TEPO/CDCl$_3$ solution as the external standard.

^{1}H spectra (30° pulse 12.25 μs, 16 scans) were referenced with the residual CHCl$_3$ signal (7.26 ppm) as the internal standard. ^{19}F spectra (30° pulse 11 μs, 128 scans) were referenced with α,α,α-trifluorotoluene (−62.7 ppm) as the internal standard.

Solid state NMR spectra were recorded in a Bruker Avance III WB400 spectrometer with 4 mm zirconia rotors spun at the magic angle in N$_2$ at 10 kHz. ^{31}P NMR spectra (64 scans) were recorded using a ^{31}P π/2 pulse length of 4.3 μs, with a spinal-64 proton decoupling sequence of 5 μs pulse length, and 30 s recycle delay. Pulses and chemical shifts were calibrated with (NH$_4$)H$_2$PO$_4$.

Results

Selection of acids, solvent and equilibration time

The objective of this study was to determine the chemical shift of the discrete isolated TEPO···H–A (1:1) species in solution, and the possible existence of the species with other stoichiometries. A set of Brønsted acids (Table 1) was selected to cover a range of acidity as wide as possible, from acetic (AcOH) and formic acids as the weakest ones, phenylphosphonic (PhPO$_3$H$_2$) and trifluoroacetic (TFA) acids as moderately strong acids, and three sulfonic acids, methanesulfonic acid (MeSO$_3$H), p-toluenesulfonic acid (pTosOH) and trifluoromethanesulfonic acid (triflic acid, TfOH) as the strongest ones. In fact, these strong acids would serve as models for different types of sulfonic solids used as heterogeneous catalysts, containing alkylsulfonic, arylsulfonic or perfluoroalkylsulfonic groups. 2,2,2-Trifluoroethanol (TFE) was also included as an example of an alcohol of high acidity.

Most of the pK_a values (Table 1) are collected from the classical reference by Guthrie,[16] with some exceptions, such as TFE,[17] PhPO$_3$H$_2$[18] and TFA.[19] A lower pK_a value of TfOH (−14.7), based on more recent theoretical calculations[20] has also been considered.

Methanol-d_4 was first envisaged as a solvent due to the rather low solubility of some acids in CDCl$_3$. However, the preliminary results obtained in methanol-d_4 (Fig. S1, ESI†) indicated that this solvent was not suitable for this kind of

Table 1 Properties of the solvents and acids used in this work

Solvent	AN^a	^{31}P $\delta_{AN}{}^a$	^{31}P $\delta_{1:1}{}^b$	p$K_a{}^c$
CHCl$_3$	23.1	52.5	—	—
MeOH	41.3	60.3	—	—
TFE	53.8	65.6	54.6	12.4
AcOH	52.9	65.2	56.5	4.76
HCOOH	83.6	78.3	57.9	3.77
PhPO$_3$H$_2$	—	—	59.3	1.83^d
TFA	105.5	87.6	62.8	0.23^e
MeSO$_3$H	126.1	96.4	74.3	−1.92
pTosOH	—	—	76.1	−2.8^f
TfOH	129.1	97.6	94.8	−5.9 (−14.7^g)

^{a} Gutmann's acceptor number and the corresponding value of ^{31}P chemical shift of dissolved TEPO. ^{b} ^{31}P chemical shift in CDCl$_3$ for a TEPO–HA (1:1) species, calculated from the slope at low acid/TEPO molar ratio. ^{c} Data from ref. 16 unless otherwise stated. ^{d} From ref. 18. ^{e} From ref. 19. ^{f} Value for benzenesulfonic acid. ^{g} From ref. 20.

24352 | *Phys. Chem. Chem. Phys.*, 2020, **22**, 24351–24358

This journal is © the Owner Societies 2020

measurement, as no shift was observed with weak acids, and no differences were observed among the strong acids, probably because the protonating species was $[CD_3ODH]^+$ in all of the cases. This effect is similar to that observed with Lewis acids and TMPO in D_2O,[14] with two general behaviors for highly active and poor catalysts. Thus, all of our studies were carried out in $CDCl_3$, as a weakly polar medium, to simulate the acid–TEPO interaction on the solids in the absence of solvent.

In spite of the presumably fast acid–base equilibrium in solution, broad unsymmetrical ^{31}P signals were obtained in some cases that became narrower single lines upon standing (some examples are collected in Fig. S2, ESI†). Hence, as a general procedure, the NMR samples were left to stand for a longer time (6–24 h) until a stable and reproducible ^{31}P spectrum was obtained.

Results with weak acids ($pK_a > 0$)

The ^{31}P chemical shift of TEPO in $CDCl_3$ was 52.5 ppm, in good agreement with the result at infinite dilution (50.8 ppm) used to determine AN.[3] The values of δ_{AN} (Table 1) have been calculated from the experimental value, according to $\Delta\delta$ reported in the literature.[1] With the different acids, the exact acid/TEPO molar ratio was determined by integration of the ^{1}H NMR spectrum, using the CH_2 signal of TEPO and some relevant signal of the acid, namely methyl groups of AcOH, $MeSO_3H$ and pTosOH, methylene group of TFE, phenyl group of $PhPO_3H_2$ and H-COOH of formic acid. In the case of $PhPO_3H_2$, the ratio was confirmed by ^{31}P NMR. Given the absence of suitable protons in the fluorinated acids (TFA and TfOH), α,α,α-trifluorotoluene was added as an internal standard and the acid/TEPO molar ratio was calculated from the integrations of both ^{1}H and ^{19}F NMR spectra.

The evolution of the ^{31}P chemical shift with the acid/TEPO molar ratio (spectra are collected in Fig. S3–S7, ESI†), in the case of weak acids, is represented in Fig. 1, showing a similar trend to the evolution of TMPO [31]P δ in D_2O with different $M(OTf)_x$/TMPO molar ratios[13] and TEPO with a different organocatalyst/TEPO ratio.[15] The slope of the curve at low acid/TEPO molar ratios should be dependent on the acid strength (curve fits are collected in Fig. S8–S12, ESI†). Using that slope, the [31]P δ values for a 1/1 molar ratio have been calculated (collected in Table 1, labeled as $\delta_{1:1}$), and they can be considered as the estimated chemical shifts for the different TEPO–HA (1:1) species. These values are in qualitative agreement with the pK_a, but they are much lower than those obtained under the Gutmann's conditions for AN calculation (δ_{AN}). At increasing acid/TEPO molar ratios, the chemical shifts slowly increase linearly to converge with δ_{AN}. This result is in contrast with previous observations where the ^{31}P chemical shift remained constant after the saturation of all of the TEPO.[15] The slope of this second line is also higher for the stronger acids, although it was not determined for $PhPO_3H_2$ and TFE due to solubility problems in $CDCl_3$. With this second straight line, it is possible to calculate a theoretical acid/TEPO ratio to get the [31]P δ_{AN}. With both acetic and formic acids, molar ratios over 50 would be required to reach the [31]P δ_{AN},
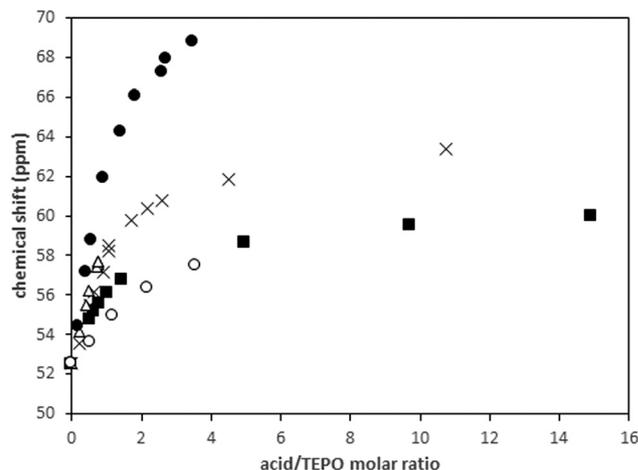

Fig. 1 Variation of the ^{31}P chemical shift (ppm) with the acid/TEPO molar ratio in $CDCl_3$: (○) TFE, (■) AcOH, (×) HCOOH, (△) $PhPO_3H_2$, (●) TFA.

indicating that a very large excess of weak acid, that is a high dilution of TEPO, is necessary to reproduce the [31]P δ_{AN} value. The molar ratio is significantly lower in the case of TFA (14.5), but a large excess is still required.

Results with strong acids ($pK_a < 0$)

Fig. 2A shows the evolution of the ^{31}P chemical shift with the acid/TEPO molar ratio in the case of strong acids (spectra are collected in Fig. S13–S15, ESI†). The general trend is analogous to that observed with weak acids, with higher initial slopes and $\delta_{1:1}$ values (Table 1). The chemical shifts for both $MeSO_3H$ and pTosOH are very similar, which is in agreement with their very close pK_a values. The trend at the higher acid/TEPO molar ratio seems to also be similar, although the data for pTosOH were limited by its rather low solubility in $CDCl_3$. In any case, the slope (curve fits are collected in Fig. S16–S18, ESI†) was higher than those observed for weak acids, and the theoretical acid/TEPO ratio to get the [31]P δ_{AN} was only 4 in the case of $MeSO_3H$.

On the contrary, the behavior of TfOH was significantly different. The $\delta_{1:1}$ value (94.8 ppm) was very close to the δ_{AN} (97.6 ppm). Hence, the second slope was much lower than that of $MeSO_3H$ (Fig. 2B). Moreover, at TfOH/TEPO molar ratios slightly higher than 1, two signals were clearly detected (open and filled symbols in Fig. 2A), until a single signal was again formed at a molar ratio of 3 (Fig. 3).

[1]H and ^{19}F spectra

The deshielding effect on TEPO was also detectable in the ^{1}H spectrum of the phosphorus neighbor methylene groups (Fig. S19, ESI†). In fact, [31]P δ and [1]H δ show a good correlation (Fig. S20, ESI†), although the ^{31}P chemical shift is much more convenient[2] due to its much wider range of variation.

The evolution of the chemical shifts in the spectra of the acids has been represented against the TEPO/acid ratio to better understand the changes from pure acid to the saturation with TEPO. In this regard, the proton donation can also be followed by ^{1}H NMR in the case of AcOH, HCOOH and $MeSO_3H$. The formyl proton

This journal is © the Owner Societies 2020
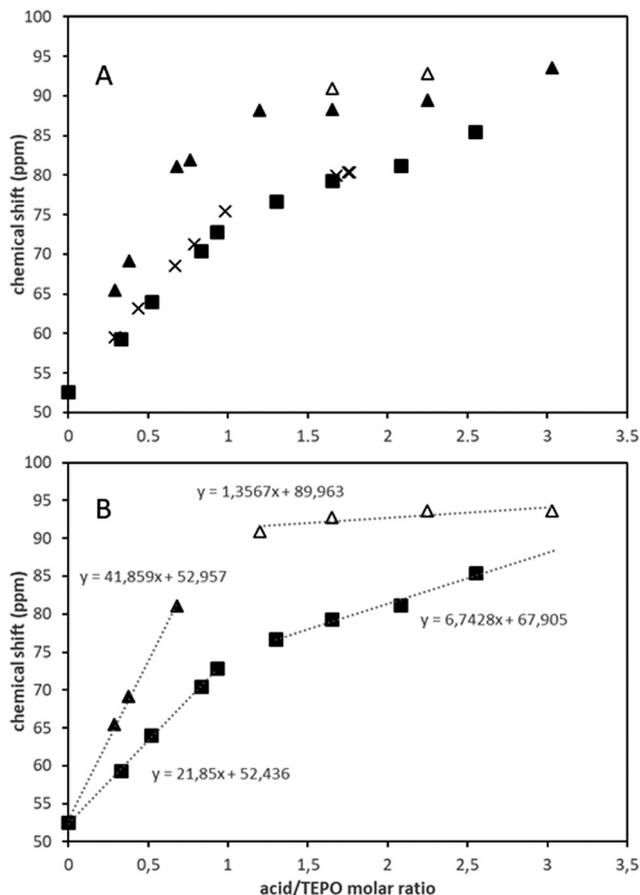
Phys. Chem. Chem. Phys., 2020, 22, 24351–24358 | 24353

Fig. 2 Variation of the ^{31}P chemical shift (ppm) with the acid/TEPO molar ratio in CDCl$_3$ (A) and linear fitting of the two straight parts of the curves (B): (■) MeSO$_3$H, (×) pTosOH, (▲△) TfOH.

Fig. 3 ^{31}P NMR spectra of TfOH–TEPO mixtures in CDCl$_3$ with different acid/TEPO molar ratios.

shows a deshielding effect (Fig. 4A and Fig. S21, ESI†) with a linear relationship with the TEPO/acid ratio, which is in agreement with the increase in the electron density in the carboxylic moiety. On the contrary, the methyl groups of the methanesulfonic (spectra in Fig. S22, ESI†) and acetic acids suffer a shielding effect (Fig. 4B and C, respectively) when the TEPO/acid molar ratio increases. This is in agreement with the development of a negative charge (an effect observed in the spectra of the sulfonate and acetate salts[21]), although the variation is much more important in the case of MeSO$_3$H. This is probably due to its stronger acidity and hence a larger proton donation degree.

The acidic proton appears in the 5–12 ppm range with variable linewidth (two examples are collected in Fig. S23 and S24, ESI†). However, no clear relationship could be found between the TEPO/acid molar ratio and the chemical shift or linewidth of the signal.

Finally, the ^{19}F chemical shift of the fluorine atoms in TFA (spectra in Fig. S25, ESI†) and TfOH follow the same trend (Fig. 5) as the protons in AcOH and MeSO$_3$H with a shielding effect at increasing amounts of TEPO. This indicates the formation of a salt, and a more intense effect in the case of the stronger acid TfOH. Moreover, a second signal is clearly
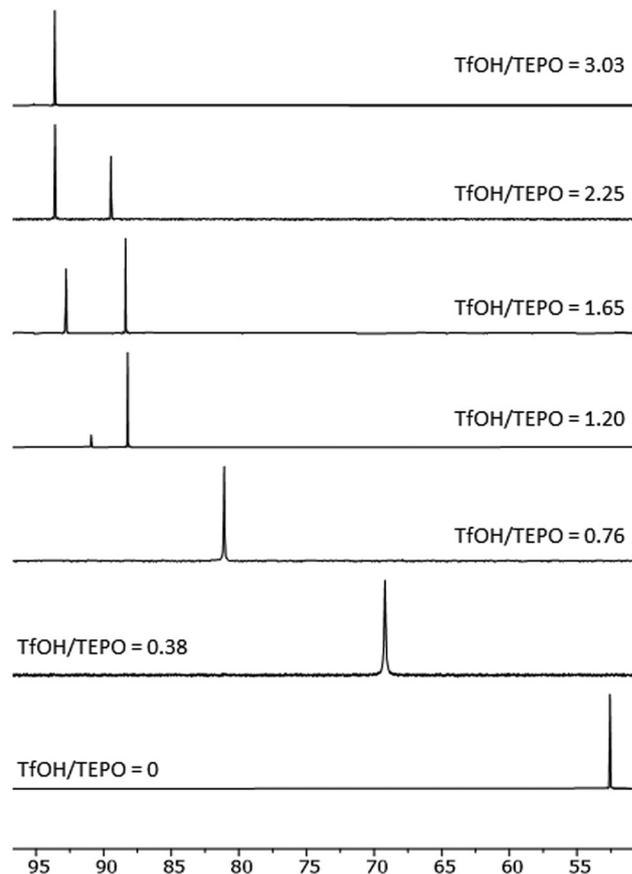
detected in the spectrum of TfOH at the same TfOH/TEPO ratios, in which the ^{31}P spectrum also shows 2 signals. This is in agreement with the formation of two different species with slow exchange rate.

Discussion

TEPO·HA species in solution

The results obtained with the set of acids at different acid/TEPO molar ratios seem to indicate a general behavior that can be summarized in Scheme 1. These equilibria are simplifications, as the presence of the acids in dimeric form[22] or higher aggregates cannot be ruled out. This should affect mainly to kinetics,[23] and it may be the reason for the required long equilibration time and the erratic chemical shift of the acidic proton. However, its role on the equilibrium position should only be marginal. At low acid/TEPO molar ratios, the major species must be free TEPO and TEPO·HA (1:1) adduct. The ^{31}P chemical shift (eqn (1)) would be dependent on the molar fractions of both species, x_{TEPO} and $x_{1:1}$, which can ideally approach the acid/TEPO molar ratio r, and their chemical shifts δ_{TEPO} and $\delta_{1:1}$:

$$\delta = \delta_{1:1}x_{1:1} + \delta_{TEPO}x_{TEPO} = \delta_{1:1}r + \delta_{TEPO}(1 - r)$$
$$= \delta_{TEPO} + r(\delta_{1:1} - \delta_{TEPO}) \qquad (1)$$

24354 | Phys. Chem. Chem. Phys., 2020, 22, 24351–24358

This journal is © the Owner Societies 2020
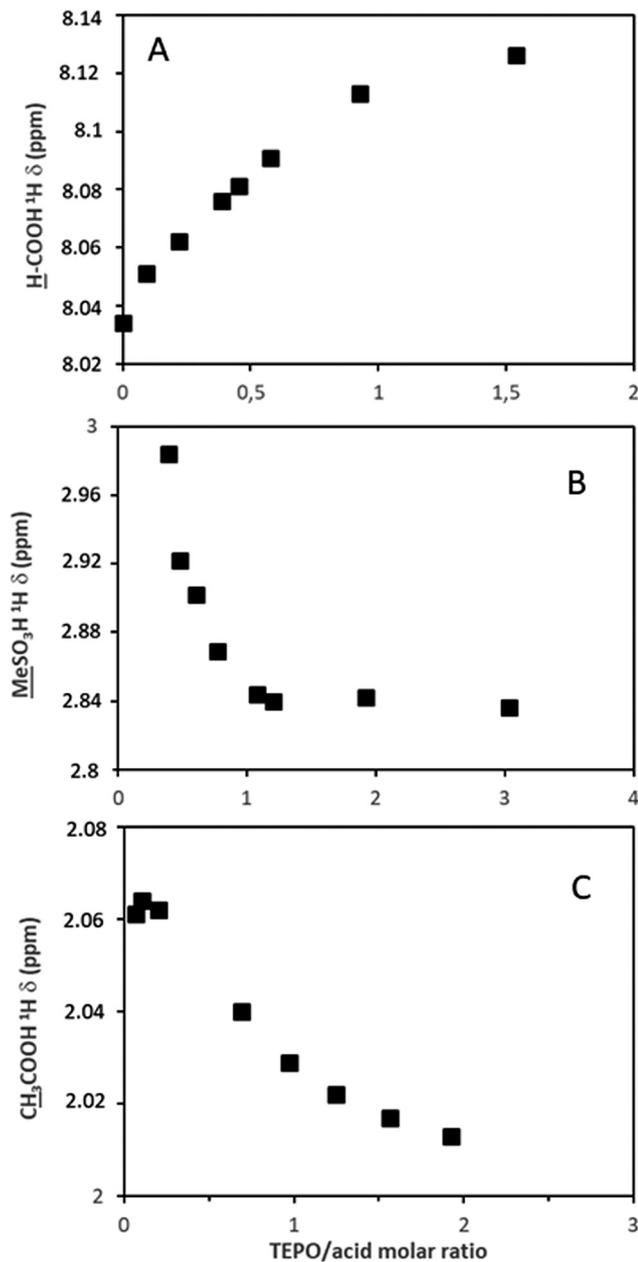
Fig. 4 Evolution of ^1H δ with TEPO/acid molar ratio: (A) H̲-COOH; (B) MeSO₃H̲; (C) M̲eCOOH.

Fig. 5 Evolution of the ^{19}F chemical shift with TEPO/acid molar ratio: (A) TFA; (B) TfOH.

Scheme 1 Proposed different acid–base equilibria of TEPO depending on the different types of acids.

In fact, the dependence of ^{31}P δ with the acid/TEPO molar ratio is always linear at low ratios (Fig. 1 and 2), and the $\delta_{1:1}$ values were calculated with the corresponding slopes (Table 1). Those values should be dependent on the strength of the acid. In fact, two different behaviors are apparent for weak and strong acids (Fig. 6). In the case of the weak acids, the increase of $\delta_{1:1}$ is very smooth with pK_a. In contrast, it rises very rapidly with strong acids. In fact, the change in trend seems to be at a pK_a value around that of TEPO ($pK_a \approx -0.5$),[24] which is similar to that of TFA.

Thus, the weak acids are not strong enough to produce the protonation of TEPO. In addition, the nature of the TEPO·HA adduct can be envisaged as a hydrogen bond of different strengths,
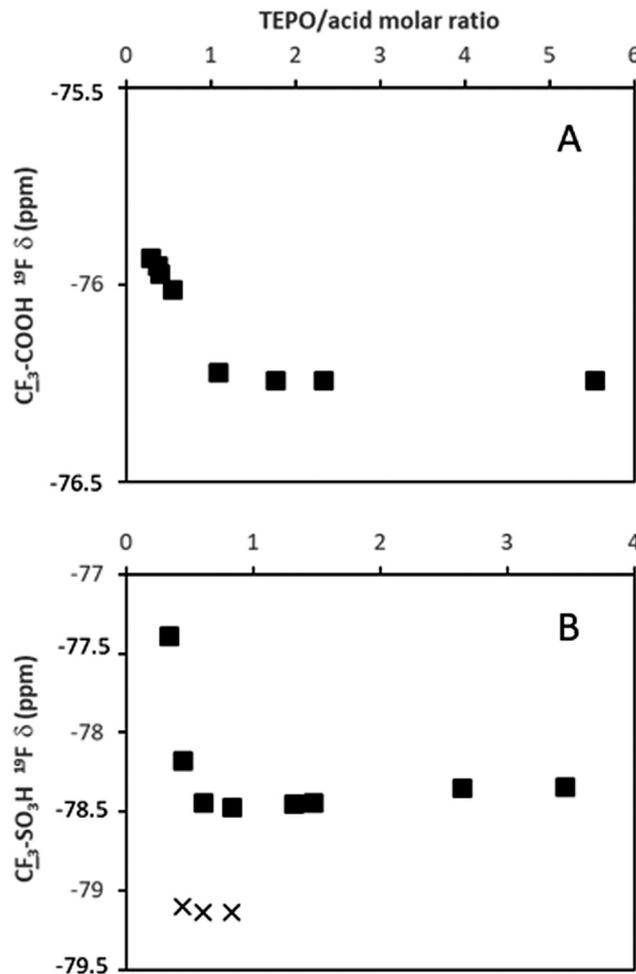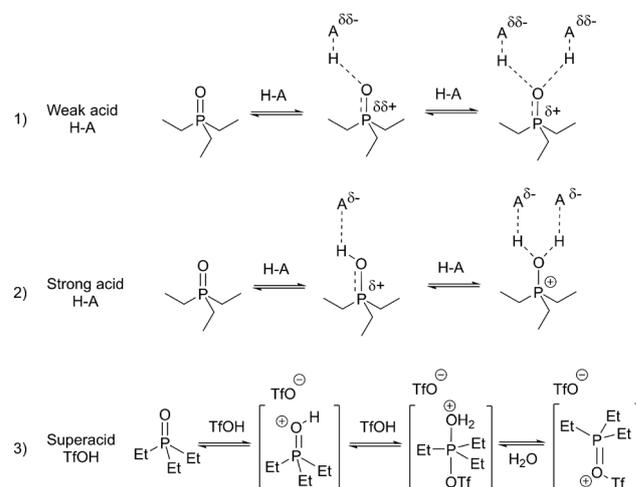
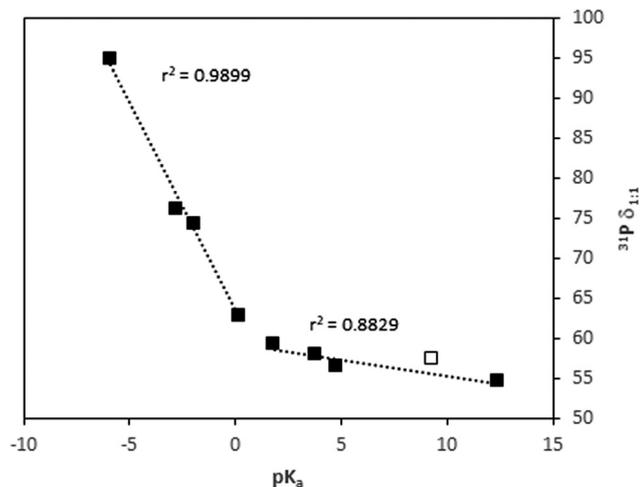in the order TFE < AcOH < HCOOH < PhPO₃H₂ < TFA. In fact, from the data reported in the literature,[15] the $\delta_{1:1}$ for

Fig. 6 Dependence of ^{31}P $\delta_{1:1}$ with pK_a (values in Table 1). Open symbol corresponds to data of HFIP from ref. 15.

Fig. 7 Evolution of the TEPO ^{31}P maximum line width with the chemical shift.

1,1,1,3,3,3-hexafluoro-2-propanol (HFIP) can be calculated (open symbol in Fig. 6), and it fits well with the expected value. The hydrogen bonding must generate only a very small positive charge on phosphorus (Scheme 1, equilibrium 1), and hence a very low deshielding effect, demonstrated by a low ^{31}P $\Delta\delta$. The acids stronger than TFA are able to transfer the proton to TEPO, developing a larger positive charge on phosphorus, and hence a more intense deshielding effect. From the $\delta_{1:1}$ values, two types of behavior can be considered. The superacid TfOH produces the complete proton transfer, forming an ion-pair with TEPO (Scheme 1, equilibrium 3). In addition, a complete deshielding effect is observed on phosphorus in the 1:1 species, as shown by a $\delta_{1:1}$ value that is very close to δ_{AN}. The strong acids MeSO$_3$H and pTosOH produce a deshielding effect that is less intense than TfOH. This is due to an incomplete proton transfer (Scheme 1, equilibrium 2), but is much more intense than the weak acids.

A second parameter that allows for distinguishing between different behaviors is the ^{31}P line width. The maximum value is always observed at an acid/TEPO ratio around 0.5, and it varies depending on the acid strength. The values are low (<10 Hz) with weak acids, indicating a fast exchange between the free and hydrogen-bonded TEPO. The maximum line width abruptly increases to values around 100 Hz when the acid strength reaches the TEPO pK_a. This is probably due to a slower exchange of the proton-transferred TEPO. The slow exchange has also been described in the case of neutralization of Lewis acids with TMPO in D$_2$O.[13] From the maximum value of the line width, it decreases in a linear way with $\delta_{1:1}$ (Fig. 7), which is with increasing acid strength. This seems to allow a faster TEPO exchange, mainly in the case of the ion-paired [TEPO–H]$^+$TfO$^-$.

The evolution of the ^{31}P δ at acid/TEPO molar ratios >1 (Fig. 1 and 2) seems to indicate the existence of a second reaction to form a TEPO–(HA)$_2$ species (Scheme 1). In the case of weak acids, this reaction should be the formation of a second hydrogen bond (Scheme 1, equilibrium 1), leading to a minor increase in δ that r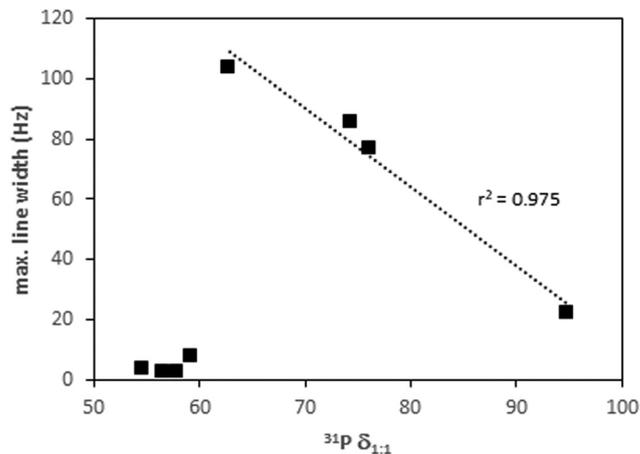equires a very high amount of acid to be detectable. On the other hand, MeSO$_3$H and pTosOH are strong enough to produce a second proton transfer to TEPO (Scheme 1, equilibrium 2), which is able to reach the full deshielding effect at a rather low acid/TEPO ratio (4:1). As TfOH already produces the full deshielding effect with the first protonation equilibrium, the second TfOH molecule might be added to the P=O bond, leading to a [Et$_3$P=OTf]OTf species after water loss (Scheme 1, equilibrium 3). This species has only a minor deshielding effect on ^{31}P with respect to [Et$_3$P=OH]OTf, and it would also explain the slow exchange, as shown by the two signals of the ^{31}P spectrum at high acid/TEPO molar ratio (Fig. 3), as well as the two signals in the ^{19}F spectrum (Fig. 5B).

Attempts to detect isolated TEPO·HA species by ^{31}P MAS NMR

In an attempt to detect the isolated 1:1 and 1:2 TEPO–HA species in the solid phase, the TEPO–HA adducts with the two solid acids, PhPO$_3$H$_2$ and pTosOH, were prepared with different acid/TEPO molar ratios to prevent the exchange process. Unfortunately, all of the mixtures, irrespective of their molar ratios, were viscous liquids at room temperature. In any case, they were imbibed with solid KBr and the spectra of the solids were recorded using MAS technique with direct polarization and proton decoupling (Fig. S26 and S27, ESI†).

A single quite narrow TEPO ^{31}P signal was obtained in all of the cases, with very low chemical shift anisotropy, as shown in the spectra at low spinning speed (up to 0.8 kHz, Fig. S28, ESI†). Then, the first conclusion was that the adducts were still present in the liquid phase on the solid surface. Even in the absence of solvent, a fast exchange of TEPO took place, averaging the signal. The obtained chemical shifts were compared with those observed in the solution phase (Fig. 8).

As can be seen, the chemical shifts at low molar ratio perfectly fit with the initial slopes of the curves in solution, showing the negligible effect of CDCl$_3$ on the chemical shift under those conditions. On the contrary, the effect is significant at molar ratios higher than 1. Conversely, the second slope (molar ratio >1) is much lower than the first one in solution. In the solvent-free liquid phase on the solid, the evolution of the chemical shift is nearly linear up to higher molar ratios.
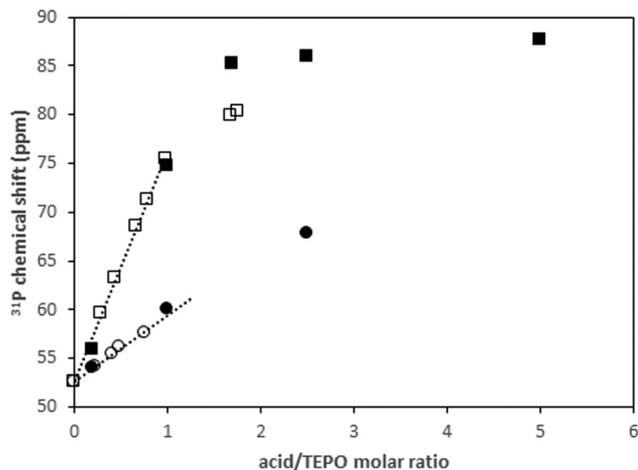
Fig. 8 Evolution of ^{31}P chemical shift in solution (open symbols) and in solid phase (filled symbols) with acid/TEPO molar ratio: (■) pTosOH; (●) PhPO$_3$H$_2$.

The concentration of the sample after evaporation of the solvent seems to greatly favor the formation of the TEPO–(HA)$_2$ species, irrespective from the acid strength.

^{31}P NMR spectra of TEPO in solution with mixtures of acids

In principle, the observed behavior of TEPO in the presence of pure acids should be useful to predict the chemical shift of TEPO in solution in the presence of a mixture of acids. One strong acid (MeSO$_3$H) and one weak acid (HCOOH) were tested with MeSO$_3$H/TEPO molar ratios that were always under 1, and different HCOOH/TEPO molar ratios. In a simple approach, the ^{31}P δ value should be a contribution of the TEPO·HO$_3$SMe species and another one of TEPO·HOOCH that is calculated using the respective $\delta_{1:1}$ and molar fractions. There would be an additional effect of the excess of acid over the acid/TEPO ratio of 1, which should be estimated with the slope of the second straight line in the δ vs. acid/TEPO ratio.

As an example, the predicted value for a MeSO$_3$H/HCOOH/TEPO ratio of 0.53 : 0.62 : 1 would be 66.6 ppm (0.53 × 74.3 + 0.47 × 57.9 + 0.15 × 0.33, where 0.33 is the slope of the second straight line in the HCOOH graphic), whereas the experimental value is 66.9 ppm.

However, the effect of a large excess of weak acid on the 1 : 1 species of the strong acid cannot be precisely predicted by the behavior of the pure weak acid. Thus, for a MeSO$_3$H/HCOOH/TEPO ratio of 0.83 : 1.03 : 1, the predicted value is 71.8 ppm, whereas the experimental one is 73.7 ppm. Even more difference is observed at larger HCOOH excess (molar ratio of 0.55 : 11.1 : 1) between the predicted δ (70.4 ppm) and the experimental value (74.0 ppm). This seems to indicate that the effect of a second molecule of the weak acid is higher when it participates in a mixed 1 : 2 species with the strong acid, although this point deserves further investigation.

Cooperative effect in diacids

If our hypothesis of the formation of the TEPO·(HA)$_2$ species is true, the effect of the second acid should be clearly observable
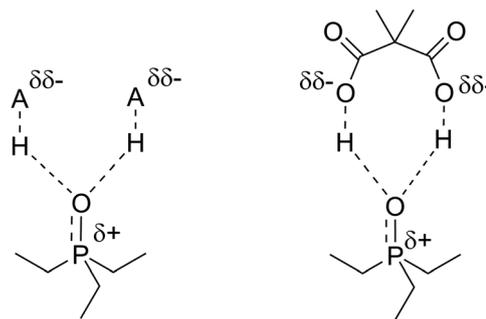

Fig. 9 Proposed structure for the TEPO·DMMA adduct and the analogous TEPO–(HA)$_2$ species with weak acids.

in the case of diacids, able to form that kind of species in an intramolecular way. Thus, dimethylmalonic acid (DMMA) was tested as an example of a carboxylic acid with a first dissociation constant higher than that of HCOOH (pK_{a1} = 3.15).[17] The solubility limitations restricted the maximum acid/TEPO molar ratio to 0.68. In that range, it was possible to calculate the $\delta_{1:1}$, which was 60.6 ppm. This was significantly higher than the value for HCOOH (57.9 ppm) and even PhPO$_3$H$_2$ (59.3), which is a stronger acid (pK_a = 1.83). This result indicates that the deshielding effect of DMMA on TEPO is larger than expected by only its pK_{a1}, which may be related to the presence of a second carboxylic acid that is able to donate a second hydrogen in an intramolecular manner (Fig. 9). This is entropically more favored than the donation from a second molecule of a simple monoacid. This result opens the way to the search for the close proximity of acid sites on heterogeneous catalysts.

Conclusions

The proportionality of the ^{31}P chemical shift of TEPO with the acid/TEPO molar ratio allows the calculation of the value for a true TEPO·acid species ($\delta_{1:1}$). In a large range of acidity, from trifluoroethanol to triflic acid (pK_a range from 12.4 to −5.9), $\delta_{1:1}$ correlates with the pK_a of the acid with different slopes for strong and weak acids. This is considered in comparison with the TEPO–H$^+$ pK_a. The difference between $\delta_{1:1}$ and the value at infinite dilution in the acid (used as a solvent, δ_{AN}), as well as the behavior of the chemical shift at acid/TEPO molar ratios >1, indicates the existence of an interaction of a second acid molecule with TEPO. This second interaction is also dependent on the acid strength, up to a limit at around 95 ppm, which seems to be the chemical shift of the TEPO–H$^+$ species, in the form of an ion-pair. The second interaction seems to be entropically highly favored in a diacid, such as dimethylmalonic acid, whose effect on the ^{31}P δ of TEPO is much more important than expected by its pK_a value.

In solids with isolated acid sites, such as in the case of zeolite HZSM-5, the formation of the (TMPO)$_2$–HA species has been proposed on the basis of ^{1}H–^{31}P HETCOR experiments and DFT calculations.[25] However, on solids with high density of acid sites, the presence of neighbor acid sites may produce an effect similar to that observed with DMMA in solution, with the

formation of the TEPO–(HA)$_2$ species. This might explain the high dispersion of the ^{31}P chemical shifts observed with the sulfonated carbons,[26] leading to an uncertain assignment of the signals,[27] a subject that requires further investigation according to these findings in solution.

Conflicts of interest

There are no conflicts to declare.

Acknowledgements

Notes and references

1 V. Gutmann, *Coord. Chem. Rev.*, 1976, **18**, 225–255.
2 I. Alkorta and J. Elguero, *J. Phys. Org. Chem.*, 2017, **30**, 1–7.
3 M. A. Beckett, G. C. Strickland, J. R. Holland and K. Sukumar Varma, *Polymer*, 1996, **37**, 4629–4631.
4 J. A. McCune, P. He, M. Petkovic, F. Coleman, J. Estager, J. D. Holbrey, K. R. Seddon and M. Swadźba-Kwasny, *Phys. Chem. Chem. Phys.*, 2014, **16**, 23233–23243.
5 R. A. Mantz, P. C. Trulove, R. T. Carlin, T. L. Theim and R. A. Osteryoung, *Inorg. Chem.*, 1997, **36**, 1227–1232.
6 S. Coffie, J. M. Hogg, L. Cailler, A. Ferrer-Ugalde, R. W. Murphy, J. D. Holbrey, F. Coleman and M. Swadźba-Kwasny, *Angew. Chem., Int. Ed.*, 2015, **54**, 14970–14973.
7 A. S. Ostras, D. M. Ivanov, A. S. Novikov and P. M. Tolstoy, *Molecules*, 2020, **25**, 1406.
8 D. Farcaşiu, A. Ghenciu and G. Miller, *J. Catal.*, 1992, **134**, 118–125.
9 J. P. Osegovic and R. S. Drago, *J. Phys. Chem. B*, 2000, **104**, 147–154.
10 A. Zheng, S. Bin Liu and F. Deng, *Chem. Rev.*, 2017, **117**, 12475–12531.
11 A. Zheng, S.-J. Huang, S.-B. Liu and F. Deng, *Phys. Chem. Chem. Phys.*, 2011, **13**, 14889–14901.
12 E. L. Myers, C. P. Butts and V. K. Aggarwal, *Chem. Commun.*, 2006, 4434–4436.
13 Y. Koito, K. Nakajima, H. Kobayashi, R. Hasegawa, M. Kitano and M. Hara, *Chem. – Eur. J.*, 2014, **20**, 8068–8075.
14 Y. Koito, K. Nakajima, R. Hasegawa, H. Kobayashi, M. Kitano and M. Hara, *Catal. Today*, 2014, **226**, 198–203.
15 K. M. Diemoz and A. K. Franz, *J. Org. Chem.*, 2019, **84**, 1126–1138.
16 J. P. Guthrie, *Can. J. Chem.*, 1978, **56**, 2342–2353.
17 *CRC Handbook of Chemistry and Physics*, ed. W. M. Haynes and D. R. Lide, CRC Press, Boca Raton, 92th edn, 2011.
18 H. H. Jaffé, L. D. Freedman and G. O. Doak, *J. Am. Chem. Soc.*, 1953, **75**, 2209–2211.
19 M. Norris, *Synlett*, 2015, 418–419.
20 A. Trummal, L. Lipping, I. Kaljurand, I. A. Koppel and I. Leito, *J. Phys. Chem. A*, 2016, **120**, 3663–3669.
21 *The Sadtler Handbook of Proton NMR Spectra*, ed. W. W. Simons, Sadtler Research Laboratories, Philadelphia, 1978.
22 J. R. Durig, L. Zhou, T. Schwartz and T. Gounev, *J. Raman Spectrosc.*, 2000, **31**, 193–202.
23 N. B. Chapman, M. R. J. Dack, D. J. Newman, J. Shorter and R. Wilkinson, *J. Chem. Soc., Perkin Trans. 2*, 1974, 971–976.
24 E. M. Arnett, E. J. Mitchell and T. S. S. R. Murty, *J. Am. Chem. Soc.*, 1974, **96**, 3875–3891.
25 C. Bornes, M. Sardo, Z. Lin, J. Amelse, A. Fernandes, M. F. Ribeiro, C. Geraldes, J. Rocha and L. Mafra, *Chem. Commun.*, 2019, **55**, 12635–12638.
26 P. A. Russo, M. M. Antunes, P. Neves, P. V. Wiper, E. Fazio, F. Neri, F. Barreca, L. Mafra, M. Pillinger, N. Pinna and A. A. Valente, *J. Mater. Chem. A*, 2014, **2**, 11813–11824.
27 P. Fernández, J. M. Fraile, E. García-Bordejé and E. Pires, *Catalysts*, 2019, **9**, 804.

24358 | *Phys. Chem. Chem. Phys.*, 2020, **22**, 24351–24358

This journal is © the Owner Societies 2020